Subproject A1.2

Light-Matter Interaction in Nano-Photonic Systems

Principle Investigator: Kurt Busch

CFN-Financed Scientists:

Further Scientists: Michael König, Paolo Longo

Institut für Theoretische Festkörperphysik
Universität Karlsruhe (TH)

Light-Matter Interaction in Nano-Photonic Systems

Introduction and Summary

In nano-photonic systems, multiple scattering and strong near-field effects significantly modify light propagation and light-matter interaction relative to ordinary systems. From a theoretical point of view, the electromagnetic field (in classical Maxwell or quantum-optical form) is then coupled to a material system that, too, may be described on several different levels of sophistication. The latter include material descriptions through linear (dispersive) refractive indices, higher-order effective nonlinear susceptibilities, and – most generally – nonlinear coupled systems dynamics where the "integrating out" of the material degrees of freedom into susceptibilities etc. is insufficient. Instead, the material's equations-of-motion have to be solved along with the corresponding field equations. The resulting effects are typically associated with rather different time and length scales and analytical solutions are available for only a few, mostly one-dimensional systems. Therefore, theoretical analyses of such systems have, in general, to be based on at least one or a combination of two rather distinct approaches: (i) numerical treatment of the linear or nonlinear electromagnetic field equations, including coupled system dynamics, and (ii) the development and subsequent analysis of appropriate effective models that capture the essential features (mostly on the material side) of the system.

Over the course of the present funding period, there has been a gradual shift of research activities within the entire project A1. The initial emphasis has been on purely dielectric nano-structures with nonlinear and/or optically active constituent materials. For instance, the former allow the formation of optical solitons and we have investigated the corresponding interaction processes. With the rise to prominence of metamaterials and plasmonic systems and the corresponding increase in questions to be answered, the initial focus has been augmented by also considering the optical properties of metallic nano-structures. For instance, rather quickly it has become clear that novel simulation methodologies should be developed. As a result, we have taken up and considerably expanded Discontinuous Galerkin methods and have applied them to several problems in metamaterials and plasmonics. By the same token, nano-fabrication techniques have matured to the point where one can reliable launch and detect single photons in an integrated optics environment. While much of the basic quantum optical phenomena have been explored in other systems, novel issues and effects may be realized in such quantum nano-optical systems. Consequently, we have started research efforts into the direction of controlling single- and few-photon transport properties in nano-photonic systems.

1. Investigations of nonlinear wave propagation and interaction processes

In periodic dielectric structures, the existence of photonic band gaps and the rich dispersive behavior near photonic band edges leads to numerous novel physical phenomena. In the presence of Kerr-nonlinear materials, the electromagnetic field intensity locally affects the refractive index of the constituent materials, which thus modifies the dispersion experienced by light. Consequently, for sufficiently intense fields nonlinear periodic structures may become transparent to electromagnetic waves with frequencies in the linear band gaps. This interplay between linear dispersion and nonlinear self-phase modulation leads to the formation of so-called Bragg- and gap-solitons which, respectively, have the major part of their spectrum outside and inside the photonic band gap [1].

Fiber Bragg gratings represent a particular promising physical realization. In these systems, the Maxwell equations are oftentimes and with considerable success reduced to an effective propagation equation for pulse envelopes – either within a nonlinear coupled mode equation (NLCME) or even a nonlinear Schrödinger equation (NLSE) approach. Now, in particular the NLSE model works reasonably well near a band edge of Bragg fiber with very weak contrast in the refractive index. However, what about system with stronger scattering on the linear level? In order to understand the limitations of the NLSE model in the context of nonlinear pulse propagation in periodic structures, we have teamed up with the group of Guido Schneider (Mathematics Department of the University Stuttgart) and have developed error estimates on the NLSE approximation to the nonlinear wave equation in one-dimensional periodic systems [2]. This analysis provides a detailed justification of the nonlinear Schrödinger equation in such systems.

A natural extension of the above works consists in the investigation of the interaction of gap solitons with point-like linear defect structures in one-dimensional systems. For instance, solitons may get pinned at such defect sites if the defect is capable of supporting nonlinear defect modes and the resulting localized excitations may be controlled in a similar fashion as the stationary gap solitons mentioned above. Clearly, the lack of translational symmetries mandates that such systems be investigated numerically using the NLCME model or an appropriate variational approach. We have carried out a detailed study of the "phase diagrams" that describe how much energy gets trapped (upper panel), transmitted (middle panel), and reflected (lower panel) when a moving soliton interacts with a point defect which, initially, is not excited [3]. The relevant control parameters are the soliton velocity and the defect strength and, depending on their actual values widely different scenarios arise. This behavior is summarized in Fig. 1.

Typical soliton-defect interaction processes associated with the different parameter regimes identified in Fig. 1 are displayed in Fig. 2. Most interestingly, the transition between the different regions can be either abrupt or continuous. For example, for small velocities and defect strengths, the transition between transmission and trapping regions is abrupt. For a given defect strength, one can easily determine a threshold velocity below which the soliton gets trapped and above which it passes through the defect. Since the NLCME model can completely be formulated in dimensionless units, our results of Figs. 1 provide a quantitative guideline to experiments on the dynamics of soliton-defect interactions in a wide range of fiber Bragg gratings.

Furthermore, a careful inspection of Fig. 1 reveals the existence of an area with a fractal pattern. This area of small soliton velocities and strong defects is marked by "A". In Fig. 3 we provide a close-up of this area where we plot the "phase diagrams" of trapped and reflected energy for velocities ranging from 0.05 to 0.15 in steps of 0.002 and defect strengths ranging from 0.85 to 1.0 in steps of 0.002. In this parameter range, transmission plays a minor role. We find irregularly alternating regions where either only reflection or both reflection and trapping takes place. In most cases, a considerable part (about 50%) of the energy gets trapped and the remaining energy is reflected. This reflection happens via multiple-bounce resonances, similar to those found in solitary wave collisions [4,5]. The resonance processes within which no energy remains trapped usually consist of only two bounces before reflection occurs. In these cases, the soliton and the defect mode appear to be in-phase, leading to complete reflection. We illustrate details of this peculiar behavior for two examples in Fig. 4.
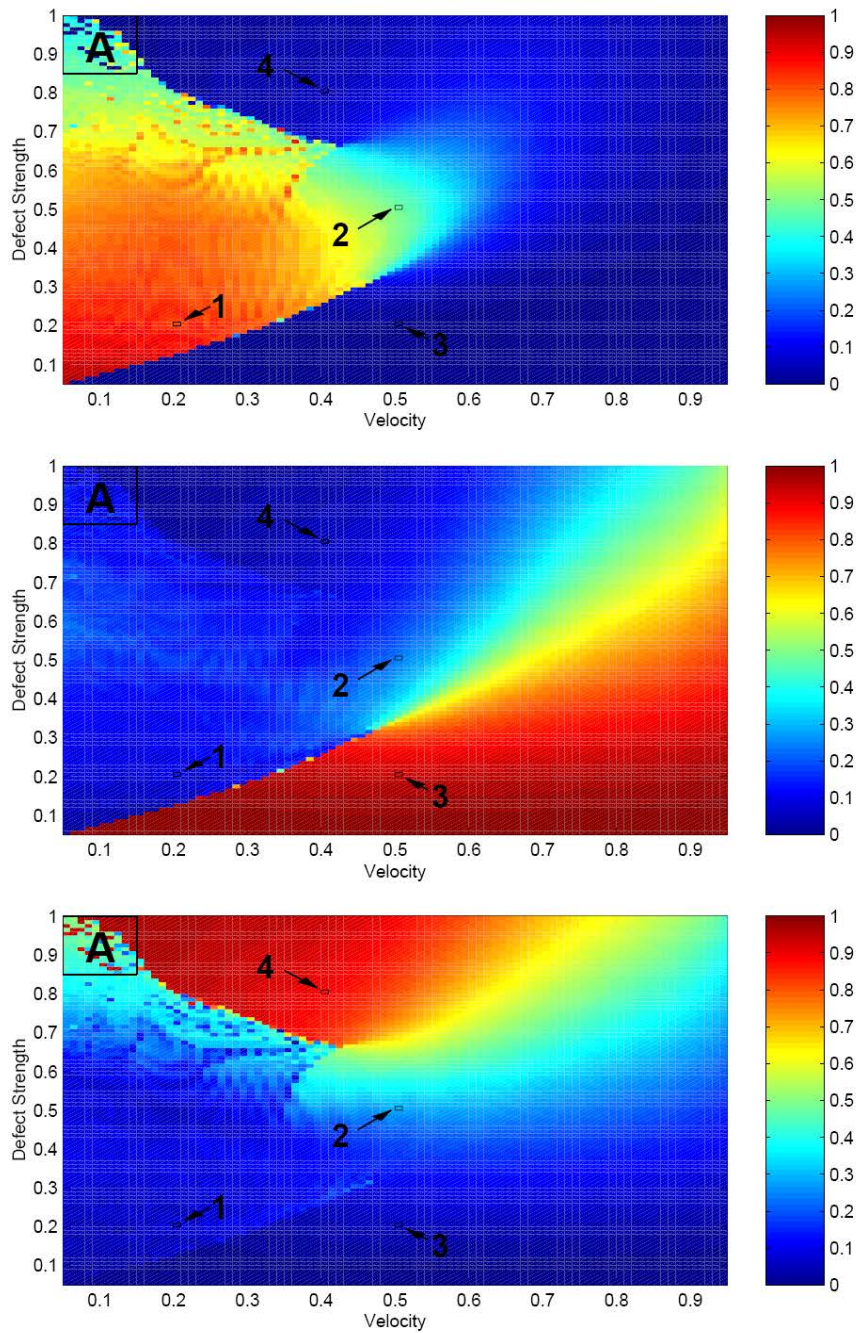
Fig.1: "Phase diagrams" of how much energy gets trapped (upper panel), transmitted (middle panel), and reflected (lower panel) when a moving soliton interacts with a point defect which, initially, is not excited. The soliton detuning is chosen such that a nonlinear defect mode could be formed. The area marked as "A" in the upper left corner of the parameter space is magnified in Fig.3. Parameters for typical processes within the various "phases" are marked with "1"-"4" and the results of the corresponding simulations are displayed in Fig.2.

(a) Trapping ($v = 0.2$, $\kappa_1 = 0.2$)

(b) Transmission ($v = 0.5$, $\kappa = 0.2$)

(c) Three-way splitting ($v = 0.5$, $\kappa = 0.5$)
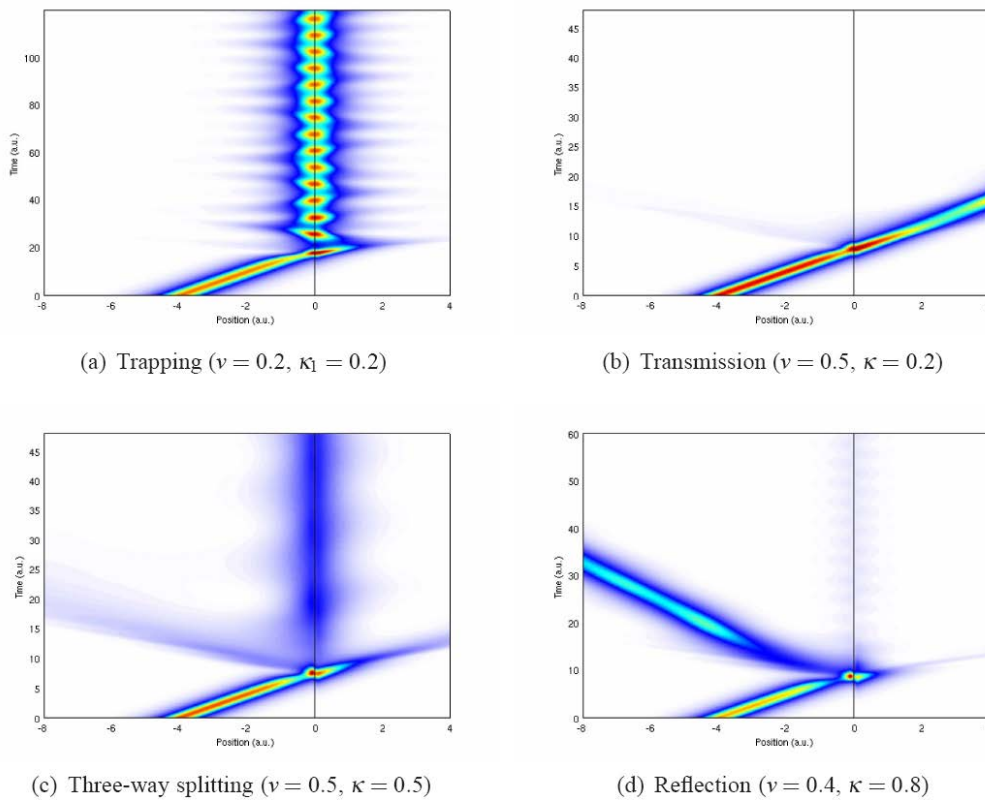
(d) Reflection ($v = 0.4$, $\kappa = 0.8$)

Fig.2: Details of typical interaction processes from the various "phases" shown in the "phase diagrams" of Fig.1. In all panels, the site of the point defect is marked with a line along the vertical time axis. The precise values of the parameters are given in the captions of the corresponding sub-figures.
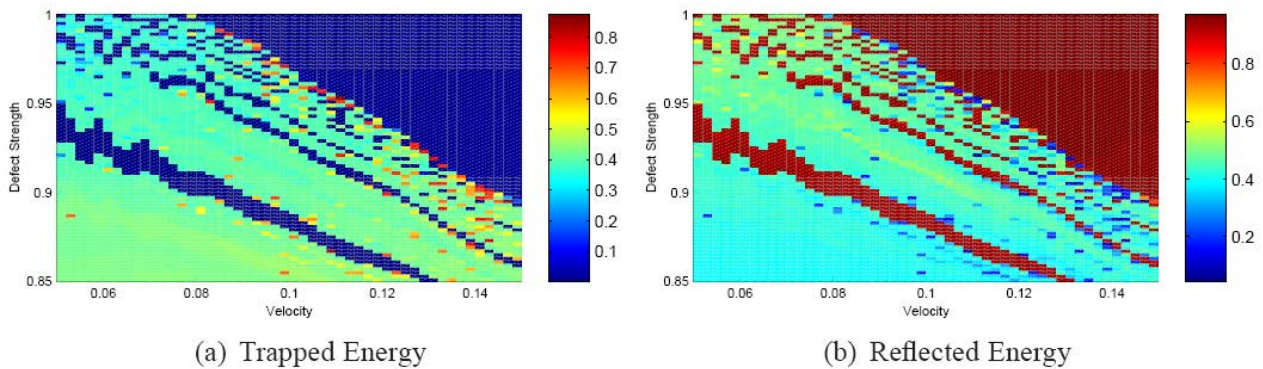

(a) Trapped Energy

(b) Reflected Energy

Fig.17: Magnification of the fractal region of parameter space denoted by "A" in the "phase diagrams" of Fig.1. Panels (a) and (b) depict, respectively, the amount of energy that is trapped and reflected when a point defect that is initially not excited is interacting with a soliton.
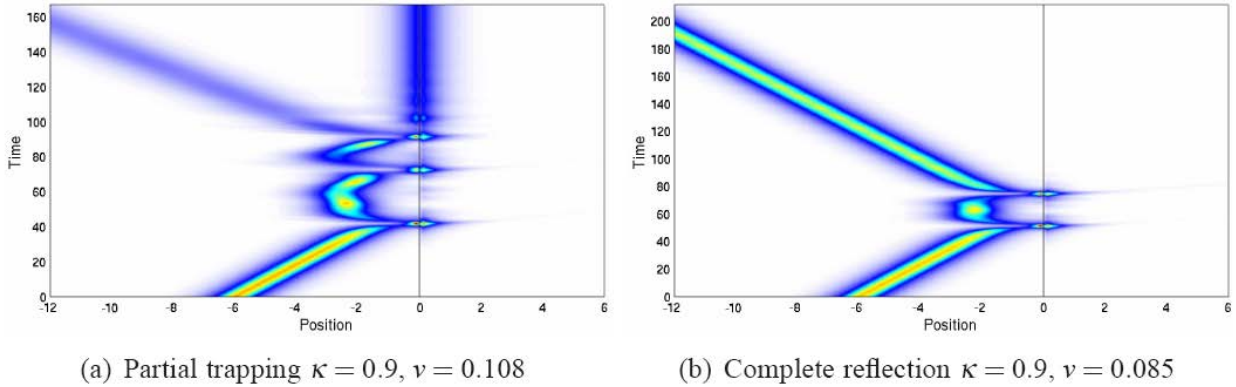
(a) Partial trapping $\kappa = 0.9, v = 0.108$ (b) Complete reflection $\kappa = 0.9, v = 0.085$

Fig.4: Details of typical interaction processes within the fractal region of the "phase diagrams" of Fig.1 and 3. In most cases about half the energy becomes trapped and the remaining part is reflected. However, for certain parameter combinations, the soliton and the defect mode appear to be in phase and all the energy is reflected.

There exist two- and multiple-bounce resonaces for this dynamical system. In particular, the two-bounce resonances lead to a situation when the energy of the reflected solitary wave is the same as the energy of the initial pulse. Iur extensive numerical simulations clearly show that the chaotic scattering of solitons is due to the multiple-bounce phenomena. This behavior is somewhat unexpected for soliton-defect interactions and certainly not anticipated from simple models such as the resonant energy transfer criterion [6] or the potential barrier model [7].

2. Metamaterials and Plasmonic Systems

The optical properties of Metamaterials and nano-plasmonic system are determined by field enhancements (and gradients thereof) associated with certain resonances of individual metallic nano-particles and interaction effects between these particles. The details of these processes such as the spectral position of resonances, the field distribution etc. depend very strongly on the details of the particles such as their shape, size and composition. In turn, this provides significant challenges to standard simulation techniques such as the venerable finite-difference time-domain (FDTD) approach. Many of these challenges can be addressed simply by moving to the frequency domain and, for instance, utilizing the flexibility of finite-element approaches regarding unstructured grids and higher-order basis functions.

Despite these apparent advantages, there exists one essential drawback that has prevented traditional finite-element methods from becoming mainstream in large-scale time-domain computations: The resulting time-stepping algorithms are implicit so that CPU-time associated with such computations quickly becomes prohibitively large even for system of moderate size. However, the past years have seen tremendous progress when Discontinuous-Galerkin (DG) finite-element techniques – originally developed for fluid dynamics – have been applied to the Maxwell equations [8]. In contrast to traditional finite-element techniques, DG-methods enforce the boundary conditions across adjacent finite elements in a weak sense through the introduction of so-called numerical fluxes. In essence, this leads to small block-diagonal mass matrices, one for each element, which may be pre-computed and inverted before the start of the actual computation. This local coupling, therefore, leads to an explicit scheme which can also easily be parallelized. In the original version [8], the time-stepping has been realized via a 4th-order low-storage Runge-Kutta scheme and the resulting simulation tool is commonly referred to as the Discontinuous-Galerkin time-domain scheme (DGTD).

6

We have realized our own implementation of DG-methods and have considerably expanded their capabilities with regard to applications in nano-photonics. At this point, we refrain from becoming too technical and only want to mention that our original extensions include the development of methods for optically anisotropic materials [9], the realization of novel types of perfectly matched layers that allow the termination of metals [10], and – in collaboration with subproject A5.6 – the development of optimized time-stepping approaches [11,12]. In addition, we have adapted certain extensions that other groups have recently developed. These include curvilinear elements and the development of a graphic-processor based version of the DGTD approach. Furthermore, we have summarized the current state-of-the-art in using DG-methods for nano-photonics in a recent review article [13].

With this powerful simulation tool, we have been able not only to address several issues in Metamaterials and plasmonic research (as described below) but also to provide crucial support for the modelling of dielectric coupled-waveguide-resonator structures [14,15]. For this latter aspect and (at present still preliminary) results on the above-mentioned graphic-processor-based implementation, we refer to the report of subproject A5.6 *Modeling of Micro-Disk Resonator Arrays*.

Regarding, metallic nano-structures, several proposals have been developed in order to realize spatio-temporal control over the localization properties of the electromagnetic field. These proposals are typically illustrated by quasi-static computations that consider only very small particles – often particles that cannot straightforwardly be fabricated in a reliable way. Therefore, we have analyzed the question of how these results translate to larger samples where (i) retardation effects could play a role and (ii) the penetration of the field is not complete because the skin depth is smaller than the particle. As expected, these issues have a detrimental effect regarding the usefulness of coherent control schemes for the spatio-temporal localization of energy but some degree of control can still be exerted [16]. In the case of extraordinary optical transmission through nano-apertures, the use of simplified material models can lead to qualitative differences with regard to realistic systems [17].

Following up on these works, we have – in collaboration with the group of Martin Wegener – applied our DG-implementation to several experimentally relevant systems [18,19,20]. In this series of works, we have been concerned with the unusual optical properties of individual split-ring resonators and their pair-wise interaction. For instance, Martin Wegener's group has been able to determine absolute values for the extinction cross-section of an individual split-ring resonator. As extinction is the combined effect of absorption and scattering, it is very interesting to determine the corresponding cross-sections separately. While this represents a serious (but not unsurmountable) challenge to experiments, the computations are rather straightforward within a total-field/scattered-field approach. The result is that the computations for the extinction cross-sections agree very well with the experimental data [18]. In addition, these computations have allowed us to decompose the extinction into absorption and scattering contributions as displayed in Fig. 5.

Based on this, we have further developed this detailed understanding of the optical properties of individual split-ring resonators further by considering the interaction effects between pairs of split-ring resonators – again in close collaboration with the group of Martin Wegener. These studies [19] show that the interaction strongly depends on the relative orientation of the split-ring resonators. As a result, the properties of entire arrays can be understood on the basis of this pair-interaction and, hence, the parameters of the array can be optimized.
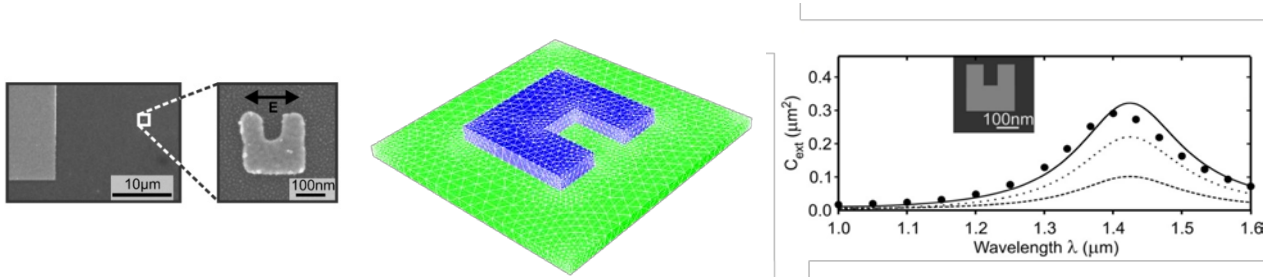
Fig.5: Left panel: SEM image of an isolated split-ring resonator (gold on glass substrate) whose extinction cross-section has been determined experimentally (dots in the right panel). Middle panel: Computational setup for the numerical determination of scattering and absorption cross-sections (dotted and dashed lines in the right panel, respectively) corresponding to the sample depicted in the left panel. Right panel: *Absolute* values for computed scattering (dotted line), absorption (dashed line), and extinction (solid line) cross-section of the setup depicted in the middle panel. The larger dots represent the results of measurements on the sample depicted in the left panel. There are no adjustable parameters in the computations.

In addition, we have recently extended the DG-approach for the computation of electron energy loss spectroscpy (EELS) [20]. Experimental EELS data allow for a spatially and spectrally mapping of plasmon modes in metallic nano-structures. Futhermore, EELS allows one to probe modes that cannot be excited optically (so-called dark modes). While these modes do not participate in radiative processes, they may be very important for the understanding the behavior of optically active material in the vicinity of metallic nano-structure, i.e., nano-antenna setups. On the one hand, these dark modes offer a non-radiative loss channel which could be detrimental for the performance of such nano-antennas. On the other hand, in spaser-type applications one actually aims for exploiting these dark modes. In Fig. 6, we illustrate the rather distinct local coupling to plasmon modes of a aluminium sphere dimer. At present, we pursue a more detailed investigation of the different modes of split-ring resonators in collaboration with the group of Stefan Linden (University of Bonn).
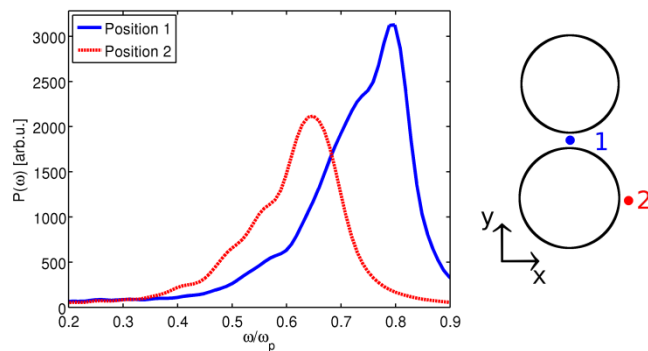

Fig.6: EELS data for a dimer of aluminum spheres (diameter 10 nm) for two different electron trajectories, labelled by 1 and 2. In case of a symmetric excitation (position 1, blue solid line), we observe a strong blue-shift of the EELS maximum relative to an excitation at an off-symmetry position (position 2, red dashed line). The single sphere plasmon resonance is around $\omega/\omega_p = 0.65$ and the corresponding dimer modes may be constructed by plasmon hybridization, i.e., the formation of "anit-binding" and "binding" dimer modes. Symmetry arguments reveal that for position 1, only the dimer's "anti-binding" mode (the optically dark mode) can be excited. For position one, both the dimer's "anti-binding" and "binding" modes (the optically dark and bright modes, respectively) can be excited.

3. Quantum Nano-Photonics

In the area of quantum photonics, high-quality single- photon sources have been developed and can readily be integrated with conventional waveguiding elements (for an overview we refer to Ref. [21]). In addition, several types of integrated optical resonators with very high quality factors such as ring resonators, disk resonators, and photonic crystal resonators have become available and may be arranged into various forms of arrays (see reports on subprojects A1.1 and A5.6). When these waveguiding structures and resonators are equipped with judiciously placed quantum-optical emitters such as quantum dots or nitrogen-vacancy centers in nano-diamond crystals, complex solid-state-based quantum optical functional elements may be realized. Consequently, much of the ongoing work aims at precisely positioning these quantum emitters within artificially structured optical materials. Similarly, in cavity and circuit QED, high-quality superconducting wave guides and cavities, strong coupling of single photons to superconducting qubits [22], and Fock states [23] have been realized for microwave photons. In addition, these waveguides and cavities may be combined with Josephson junctions and several of these compound elements may be arranged to form left- and right-handed transmission lines that exhibit tunable dispersion relations. Finally, suitably engineered Josephson junctions realize few-level quantum systems for microwave photons whose coupling strength to the radiation field can be tuned to values that are simply not available in traditional quantum-optical systems at optical frequencies.

Despite the apparent disparity in operation wavelengths and underlying physical system, the common goal of all the above approaches is the realization of integrated quantum optical devices that operate in the few-photon regime. This includes but is not limited to the more specific goals of efficient generation and detection of single photons (or even plasmons), the realization and control of effective photon-photon interaction processes, the generation and control of photon entanglement, with the ultimate goal of the realizing complex quantum-optical functional elements and devices. As most of such high-quality samples and systems have become available only recently, there exists a rather limited number of theoretical works that explore the potential of such systems with regards to modifying light-matter interaction and its utilization for realizing and controlling the above effective light-light interaction processes. Similar to the early works by Fano, which have been concerned with a discrete (electronic) state that interacts coherently with a continuum of (electronic) states [24], we may expect interesting physics to occur in the quantum photonic case as well. Obviously, the details will depend on the emitter, its interaction with the continuum and – quite important for the photonic case as it can be engineered – the structure of the continuum itself.

Therefore, we have – in close collaboration with Peter Schmitteckert (subproject B2.10 *Time-Dependent Electron Transport through Nanostructures*) – developed a computational framework that allows us to investigate few-photon transport processes in real time and real space [25]. This facilitates a direct monitoring of the interaction processes and the computation of experimentally relevant quantities, notably correlation functions. It turns out that the finite bandwidth associated with typical waveguiding systems leads to the formation of bound single-particle (photon-atom) states when a quantum impurity is coupled to the waveguide even when the impurity's transition energy is in the continuum of waveguiding modes. Thus, this state cannot be excited via single-photon processes as it is energetically forbidden. Nevertheless, the fermionic nature of this bound state (derived from the fermionic nature of the quantum impurity, say, a two-level atom) in conjunction with the bosonic nature of the waveguiding modes allows for a different scenario: An incoming few-photon wave packet my temporarily saturate the impurity and thus induce nonlinear scattering processes which allow an excitation of the bound photon-atom state. Once the wave packet has left the impurity this excitation (and de-excitation) channel ceases to exist and the

partially excited bound state remains [26] – corresponding to a trapping of radiation at the impurity side as well as an entanglement between the transmitted and reflected part of the wave packet. Based on the nonlinear nature of these processes, a considerable degree of control can be exerted by controlling the local intensity on the few-photon level.
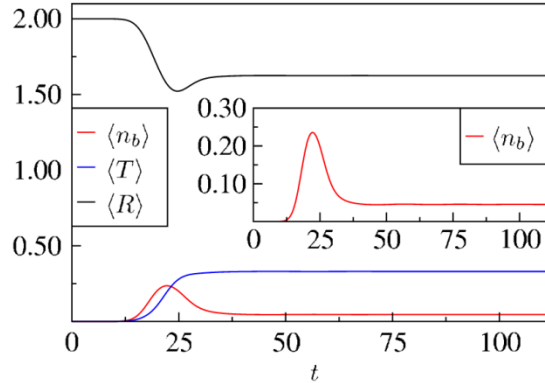

Fig.7: Time evolution (in units of $\hbar/J$) of transmission T, reflection R, and impurity occupation n_b for a two-photon wave packet that scatters at a two-level quantum impurity. The impurity has a transition energy $\Omega = \sqrt{2}$ J and couples with coupling strength V = J to the central lattice site $x_0 = 100a$ of a tight-binding lattice with total extent L = 199a hopping element J. The photons are described via boson-symmetric wave packets that are constructed from single-particle Gaussian wave functions of width s = 6a with wave number k = $3\pi/4a$ and initial center x_c = 70a. All computations are stopped at times not exceeding the transit time, i.e., the time the wave packet needs to pass through the waveguide, thus avoiding artificial reflections from the system's boundaries.

This is illustrated in Fig. 7, where we display the temporal evolution of transmission, reflection and impurity occupation for a two-photon wave packet that propagates within a one-dimensional waveguide with cosine-type dispersion relation and scatters at a two-level quantum impurity. Apparently, a sizeable amount of radiation is trapped at the impurity site. Similar computations with a single-photon wave packet show a complete decay of the impurity occupation [25]. This confirms that the bound photon-atom state has been excited by nonlinear scattering processes on the few-photon level. Finally, we would like to emphasize the generality of our approach which is capable of treating systems with arbitrary dispersion relations and atom-field coupling strengths both in real and momentum space. Thus, the trapping of the photon population and its control suggest that such systems may be exploited for engineering photon entanglement as well as for the realization of quantum logic circuits in a number of systems that range from silicon integrated optical elements all the way to superconducting quantum circuits for microwave photons..

References

- own work with complete titles -

[1] C. M. de Sterke and J. E. Sipe, in E. Wolf (Ed.), Progress in Optics **XXXIII**, 203 (1994)
[2] K. Busch, G. Schneider, L. Tkeshelashvili, and H. Uecker, *Justification of the nonlinear Schrödiger equation in spatially periodic media*, Z. angew. Math. Phys. **57**, 905 (2006)
[3] J. Niegemann, L. Tkeshelashvili, and K. Busch, *Chaotic scattering of solitons on point defects in fiber Bragg gratings*, Optics Express **16**, 10170 (2008)
[4] R. H. Goodman and R. Haberman, SIAM J. Appl. Dyn. Syst. **4**, 1195 (2005)

[5] R. H. Goodman and R. Haberman, Phys. Rev. Lett. **98**, 104103 (2007)

[6] R. H. Goodman, R. E. Slusher, and M. Weinstein, J. Opt. Soc. Am. B **19**, 1635 (2002).

[7] W. C. K. Mak, B. A. Malomed, and P. L. Chu, J. Opt. Soc. Am. B **20**, 725 (2003)

[8] J. Hesthaven and T. Warburton, J. Comput. Phys. **181**, 186 (2002)

[9] M. König, K. Busch, and J. Niegemann, *The Discontinuous Galerkin Time-Domain Method for Maxwell's Equations with Anisotropic Materials*, Photonics Nanostruct. **8**, 303 (2010)

[10] M. König, C. Prohm, K. Busch, and J. Niegemann, *Stretched-coordinate PMLs for Maxwell's equations in the discontinuous Galerkin time-domain method*, Opt. Express **19**, 4618 (2011)

[11] R. Diehl, K. Busch, and J. Niegemann, *Comparison of low-storage Runge-Kutta schemes for Discontinuous-Galerkin Time-Domain simulations of Maxwell's Equations*, J. Comput. Theor. Nanosci. **7**, 1572 (2010)

[12] J. Niegemann, R. Diehl, and K. Busch, *Efficient low-storage Runge-Kutta schemes with optimized stability regons*, J. Comput. Phys., in press (2011)

[13] J. Niegemann, M. König, and K. Busch, *Discontinuous Galerkin methods in nanophotonics*, Laser & Photonics Reviews, in press (2011); doi:10.1002/lpor.201000045

[14] Niegemann, W. Pernice, and K. Busch, *Simulation of Optical Resonators using DGTD and FDTD*, J. Opt. A **11**, 114015 (2009)

[15] K.R. Hiremath, J. Niegemann, and K. Busch, *Analysis of light propagation in slotted resonator based systems via coupled-mode theory*, Opt. Express **19**, 8641 (2011)

[16] K. Stannigel, M. König, J. Niegemann, and K. Busch, *Discontinuous Galerkin time-domain computations of metallic nanostructures*, Opt. Express 17, 14934 (2009)

[17] J. Niegemann, M. König, K. Stannigel, and K. Busch, *Higher-Order Time-Domain Methods for the Analysis of Nano-Photonic Systems*, Photonics Nanostruct. **7**, 2 (2009)

[18] M. Husnik, M.W. Klein, N. Feth, M. König, J. Niegemann, K. Busch, S. Linden, and M. Wegener, *Absolute Extinction Cross Section of Individual Magnetic Split-Ring Resonators*, Nature Photonics **2**, 614 (2008)

[19] N. Feth, M. König, M. Husnik, K. Stannigel, J. Niegemann, K. Busch, M. Wegener, and S. Linden, *Electromagnetic interaction of split-ring resonators: The role of separation and relative orientation*, Opt. Express **18**, 6545 (2010)

[20] C. Matyssek, J. Niegemann, W. Hergert, and K. Busch, *Computing electron energy loss spectra with the Discontinuous Galerkin Time-Domain method*, Photonics Nanostruct., in press (2011); doi:10.1016/j.photonics.2011.04.003

[21] C. Santori, D. Fattal, and Y. Yamamoto, Single-Photon Devices and Applications (Wiley-VCH, Weinheim, Germany, 2010)

[22] A. Wallraff, D. I. Schuster, A. Blais, L. Frunzio, R.-S. Huang, J. Majer, S. Kumar, S. M. Girvin, and R. J. Schoelkopf, Nature **431**, 162 (2004)

[23] M. Hofheinz, E. M. Weig, M. Ansmann, R. C. Bialczak, E. Lucero,M. Neeley, A. D. O'Connell, H.Wang, J.M.Martins, and A. N. Cleland, Nature **454**, 310 (2008)

[24] U. Fano, Nuovo Cimento **12**, 154 (1935); Phys. Rev. **124**, 1866 (1961)

[25] P. Longo, P. Schmitteckert, and K. Busch, *Dynamics of photon transport through quantum impurities in dispersion-engineered one-dimensional systems*, J. Opt. A **11**, 114009 (2009)

[26] P. Longo, P. Schmitteckert, and K. Busch, *Few-photon transport in low-dimensional systems: Interaction-induced radiation trapping*, Phys. Rev. Lett. **104**, 023602 (2010)